

Title : will be set by the publisher
Editors : will be set by the publisher
EAS Publications Series, Vol. ?, 2020

PIERNIK MHD CODE — A MULTI-FLUID, NON-IDEAL EXTENSION OF THE RELAXING-TVD SCHEME (I)

Michał Hanaasz¹, Kacper Kowalik¹, Dominik Wóltański¹ and Rafał Pawłaszek¹

Abstract. We present a new multi-fluid, grid MHD code PIERNIK, which is based on the Relaxing TVD scheme. The original scheme has been extended by an addition of dynamically independent, but interacting fluids: dust and a diffusive cosmic ray gas, described within the fluid approximation, with an option to add other fluids in an easy way. The code has been equipped with shearing-box boundary conditions, and a selfgravity module, Ohmic resistivity module, as well as other facilities which are useful in astrophysical fluid-dynamical simulations. The code is parallelized by means of the MPI library. In this paper we shortly introduce basic elements of the Relaxing TVD MHD algorithm, following Trac & Pen (2003) and Pen *et al.* (2003), and then focus on the conservative implementation of the shearing box model, constructed with the aid of the Masset's (2000) method. We present results of a test example of a formation of a gravitationally bounded object (planet) in a self-gravitating and differentially rotating fluid.

1 Introduction — the basic Relaxing TVD scheme

The **Relaxing-TVD** conservative scheme (Jin & Xin 1995) presented by Trac & Pen (2003) and Pen *et al.* (2003), who provided short codes with a basic implementation of the method, is a second order algorithm in space and time. The scheme efficiently deals with shocks without artificial viscosity. The code is very flexible and can be extended with new modules representing additional physical processes. The simplicity and robustness of the code is reflected in general performance of 10^5 zone-cycles/s (on 2 GHz AMD Opteron processors).

The conservative form of MHD equations serves as a starting point

$$\partial_t \mathbf{u} + \partial_x \mathbf{F}(\mathbf{u}, \mathbf{B}) + \partial_y \mathbf{G}(\mathbf{u}, \mathbf{B}) + \partial_z \mathbf{H}(\mathbf{u}, \mathbf{B}) = 0. \quad (1.1)$$

¹ Toruń Centre for Astronomy, Nicolaus Copernicus University, Toruń, Poland;
e-mail: mhanasz@astri.uni.torun.pl

where $\mathbf{u} = (\rho, m_x, m_y, m_z, e)$ and $\mathbf{F}(\mathbf{u}, \mathbf{B})$, $\mathbf{G}(\mathbf{u}, \mathbf{B})$, $\mathbf{H}(\mathbf{u}, \mathbf{B})$ are fluxes of the conserved fluid variables in x , y and z directions, respectively. Other symbols have their common meaning i.e. ρ denotes density of the fluid, whereas m_x , m_y , m_z are components of momentum density and e stands for total energy density.

Firstly, a dimensional splitting of equation (1.1) is made by constructing numerical solution with timestep Δt to the equation

$$\partial_t \mathbf{u} + \partial_x \mathbf{F}(\mathbf{u}, \mathbf{B}) = 0, \quad (1.2)$$

separately for each dimension. Then \mathbf{u} and \mathbf{F} are split into waves that propagate leftwards and rightwards

$$\mathbf{u}^L \equiv \frac{1}{2} \left(\mathbf{u} - \frac{\mathbf{F}}{c} \right), \quad \mathbf{u}^R \equiv \frac{1}{2} \left(\mathbf{u} + \frac{\mathbf{F}}{c} \right), \quad \mathbf{u} = \mathbf{u}^L + \mathbf{u}^R, \quad (1.3)$$

$$\mathbf{F}^L = c\mathbf{u}^L, \quad \mathbf{F}^R = c\mathbf{u}^R, \quad \mathbf{F} = \mathbf{F}^R + \mathbf{F}^L \quad (1.4)$$

where c , called the *freezing speed*, is a function that satisfies $c \geq \max(|v \pm c_f|)$, v is the fluid speed and c_f is the fast magnetosonic speed. Now, equation (1.2) is equivalent to two independent equations:

$$\partial_t \mathbf{u}^L - \partial_x \mathbf{F}^L = 0, \quad \partial_t \mathbf{u}^R + \partial_x \mathbf{F}^R = 0. \quad (1.5)$$

The above pair of equations (1.5) is solved by means of an upwind conservative scheme, separately for right- and left-going waves, using cell-centered fluxes. To achieve 2nd order spatial accuracy, a monotone upwind interpolation of fluxes onto cell boundaries is made, with the aid of a *flux limiter*. Second order accuracy of time integration is achieved through the Runge-Kutta scheme (details see Trac & Pen 2003, Pen *et al.* 2003)

2 Source terms

In order to incorporate gravity we modified the original Relaxing TVD scheme through the addition of source terms within the Runge-Kutta algorithm. To achieve a good accuracy in simulations of near-hydrostatic equilibrium states, the gravity source terms are computed separately for the left- and right-going waves, by replacing zeros on the rhs. of eqns. (1.5) by the gravity source terms $S(u^L) = (0, g_x^L \rho^L, g_y^L \rho^L, g_z^L \rho^L, \mathbf{g}^L \cdot \mathbf{m}^L)$ and $S(u^R) = (0, g_x^R \rho^R, g_y^R \rho^R, g_z^R \rho^R, \mathbf{g}^R \cdot \mathbf{m}^R)$. The superscripts ‘L’ and ‘R’ in the gravitational acceleration reflects the fact that \mathbf{g} is interpolated in a slightly different manner for the left-going and right-going waves.

3 Constrained Transport

The original RTVD MHD scheme by Pen *et al.* (2003) incorporates magnetic field evolution through the “constrained transport” (CT) algorithm (Evans *et al.* 1988).

Magnetic field \mathbf{B} is updated during the advection–constraint steps. The electromotive force is computed in the advection step by the RTVD scheme and then used in the constraint step to preserve $\nabla \cdot \mathbf{B} = 0$ (Pen *et al.* 2003).

Our extension of the RTVD algorithm includes an unsplit evolution of magneto–fluid, i.e. the simultaneous update of fluid variables and magnetic field in each Runge–Kutta step.

4 Parallelization

Piernik–MHD is fully parallelized with the aid of MPI library, by means of the block decomposition. Computational domain can be divided into any number of equal size blocks in any direction (see fig. 1). A test of code scalability has been

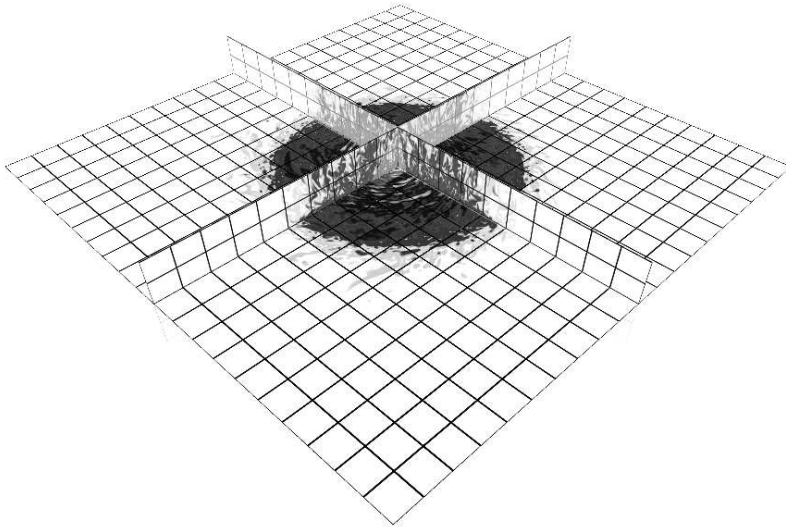


Fig. 1. Total magnetic field in a global simulation of CR–driven galactic dynamo. The computational domain is divided into 1600 ($20 \times 20 \times 4$) equal blocks.

done for HD Sedov explosion, in a series of experiments for different numbers of fixed size ($n_x = n_y = n_z = 64$) MPI blocks, distributed over different CPU cores. The results displayed in Fig. 2 demonstrate that the growth of the core number from 8 up to 1024 results in the growth of the wall time only by a few percent. As it is apparent, the simplicity and homogeneity of the grid decomposition results in an excellent scaling of the code.

5 Shearing box

In addition to the standard shearing model (Hawley *et al.* 1995), we implemented a modification of the shearing box method that allows to get rid of the

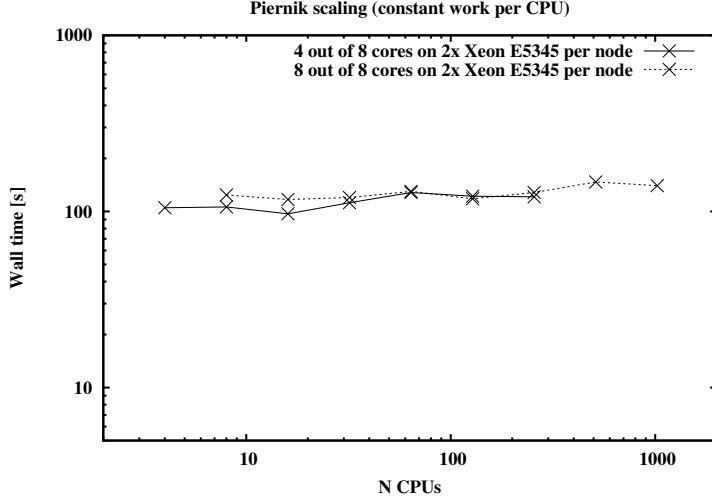


Fig. 2. Results of the weak scaling test. In each test one CPU core processed one MPI block of fixed size ($n_x = n_y = n_z = 64$).

average shear velocity ($\bar{v} = -q\Omega_0 x$) when applying the CFL condition. Firstly, we make a simple transformation of initial conservative variables

$$\mathbf{u} = (\rho, \rho v_x, \rho v_y, \rho v_z, e) \implies \tilde{\mathbf{u}} = (\rho, \rho v_x, \rho \tilde{v}_y, \rho v_z, \tilde{e}), \quad (5.1)$$

where $\tilde{v}_y = v_y - \bar{v}$, $\tilde{e} = e - \frac{1}{2}\rho(\bar{v}^2 + 2\tilde{v}_y\bar{v})$ are quantities deprived of the terms containing mean shear flow. It can be shown that the transformation (5.1) does not break the conservative form of basic HD equations

$$\partial_t \tilde{\mathbf{u}} + \partial_x \mathbf{F}(\tilde{\mathbf{u}}, v_x) + \partial_y \mathbf{G}(\tilde{\mathbf{u}}, v_y) + \partial_z \mathbf{H}(\tilde{\mathbf{u}}, v_z) = \mathbf{S}. \quad (5.2)$$

Following the fast Eulerian transport algorithm for differentially rotating disks introduced by Masset (2000) we can rewrite (5.2) as

$$\partial_t \tilde{\mathbf{u}} + \partial_x \mathbf{F}(\tilde{\mathbf{u}}, v_x) + \partial_y \tilde{\mathbf{G}}(\tilde{\mathbf{u}}, \tilde{v}_y) + \partial_z \mathbf{H}(\tilde{\mathbf{u}}, v_z) + \bar{v} \partial_y \tilde{\mathbf{u}} = \tilde{\mathbf{S}}. \quad (5.3)$$

The algorithm solving the equation (5.3) is then split into three steps:

1. computation of source terms $\tilde{\mathbf{S}}(\tilde{\mathbf{u}})$,
2. transport of $\tilde{\mathbf{u}}$ in x , y and z directions with v_x, \tilde{v}_y, v_z accordingly

$$\partial_t \tilde{\mathbf{u}} + \partial_x \mathbf{F}(\tilde{\mathbf{u}}, v_x) + \partial_y \tilde{\mathbf{G}}(\tilde{\mathbf{u}}, \tilde{v}_y) + \partial_z \mathbf{H}(\tilde{\mathbf{u}}, v_z) = \tilde{\mathbf{S}}, \quad (5.4)$$

using RTVD scheme,

3. transport of $\tilde{\mathbf{u}}$ in y with \bar{v} described by the linear advection equation

$$\partial_t \tilde{\mathbf{u}} + \bar{v} \partial_y \tilde{\mathbf{u}} = 0, \quad (5.5)$$

The linear advection equation is being solved by the means of Fast Fourier Transform (FFT). Fluid variables are transformed into the frequency domain along y direction and phase shifted of $\phi = \bar{v}\Delta t$. The algorithm is now being extended to MHD equations in a manner preserving $\nabla \cdot \mathbf{B} = 0$ (Johnson *et al.* 2008).

6 Selfgravity

We have implemented a Poisson solver in order to incorporate selfgravity of the fluids. Currently, our code supports selfgravity under condition of periodicity (or quasi-periodicity) of the domain in two or three directions, as our solver is based on FFT techniques. Utilisation of FFT is fully consistent with the previously described shearing box model. Poisson equation is solved in the shearing box by (1) the phase shift of the domain into the nearest periodic point (1D FFT in y), (2) application of suitable algorithm for periodic boundary conditions (two 1D FFT in x), (3) shift back of the calculated gravitational potential (one 1D FFT).

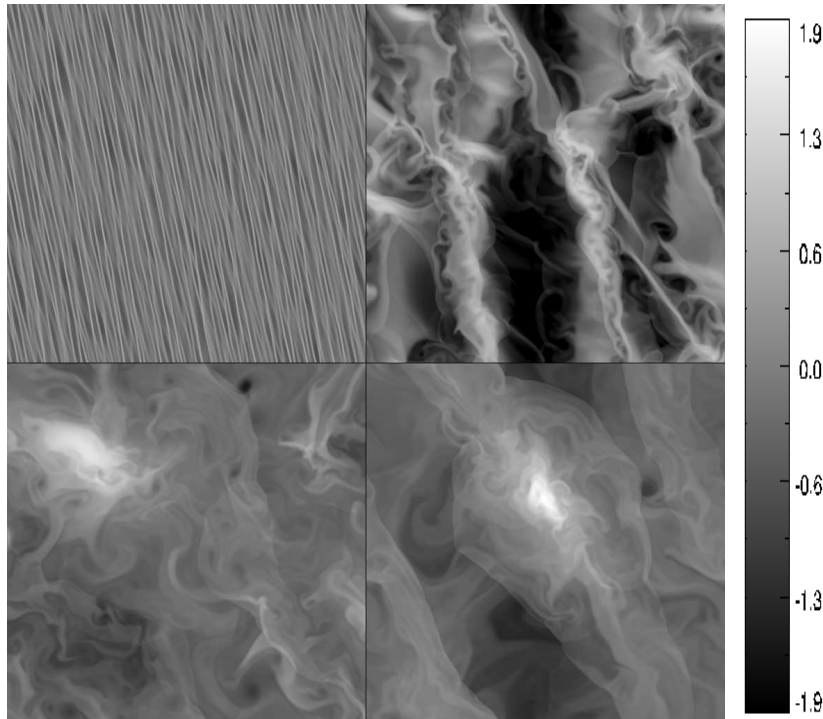


Fig. 3. Snapshots of logarithm of surface density for times $t = 3, 5, 9, 30\Omega^{-1}$. Initially marginally stable state is slightly disturbed and undergoes fragmentation. Due to high cooling rate gas collapses to one gravitationally bounded object.

The new, efficient shearing box algorithm has been tested in simulations of

gravitational instability in protoplanetary disks (Kowalik 2008). Following Gammie (2001) we set initially uniform density distribution of ideal gas ($\gamma = 2$) with a subsonic ($0.01c_s$) velocity perturbation. Depending on how efficient the cooling of the gas is, fragmentation to gravitationally bounded object or gravitoturbulence may occur. Our results correspond closely to the results of a similar approach that uses a non-conservative scheme (Gammie 2001; Brandenburg & Dobler 2002).

Acknowledgements

This work was partially supported by Nicolaus Copernicus University through Rector's grant No. 516-A, by European Science Foundation within the ASTROSIM project and by Polish Ministry of Science and Higher Education through the grants 92/N-ASTROSIM/2008/0 and PB 0656/P03D/2004/26.

References

- Brandenburg, A., Dobler, W. 2002, *Comp. Phys. Comm.*, 147, 471
Evans, C.R., Hawley, J.F. 1988, *ApJ*, 332, 659
Gammie, C.F. 2001, *ApJ*, 553, 174
Gottlieb, S., Shu, C.-W., Tadmor, E. 2001, *SIAM Review*, 43, 89
Hawley, J.F., Gammie, C.F., Balbus, S.A., 1995, *ApJ*, 440, 742
Jin, S., Xin, Z. 1995, *Comm. Pure Appl. Math.*, 48, 235
Johnson, B.M., Guan, X., Gammie, C.F. 2008, *ApJS*, 177, 373
Kowalik, K. 2008, *Master thesis at Nicolaus Copernicus University*
Masset, F. 2000, *A&AS*, 141, 165
Pen, U.-L., Arras, P., Wong, S. 2003, *ApJS*, 149, 447
Schiesser, W.E. 1991, *The Numerical Method of Lines*, Academic Press
Trac, H., Pen, U.-L. 2003, *PASP*, 115, 303